Desalination and Water Treatment
www.deswater.com

doi: 10.5004/dwt.2023.29287

284 (2023) 159–164
February

Adsorption of cesium ion by Prussian blue filled in tube-in-tube hollow fiber membranes

Shengnan Fan[a], Lu Jiang[a], Zhiqian Jia[a,*], Yu Yang[b,*], Li'An Hou[b,c,*]

[a]*College of Chemistry, Beijing Normal University, Beijing 100875, China, emails: zhqjia@bnu.edu.cn (Z. Jia), 202021150048@mail.bnu.edu.cn (S. Fan), 853761077@qq.com (L. Jiang)*
[b]*School of Environment, Beijing Normal University, Beijing 100875, China, emails: yangyu@bnu.edu.cn (Y. Yang), houla@cae.cn (L. Hou)*
[c]*High Tech Inst Beijing, Beijing, 100000, China*

Received 14 March 2022; Accepted 22 December 2022

ABSTRACT

^{137}Cs and other radionuclides in the wastewater of nuclear energy have caused great harm to the environment and human body. Removed of these radionuclides has become one of focuses of research. Prussian blue (PB), as an excellent adsorbent for cesium ion, faces the difficulty in recovery from water after adsorption. In this article, PB powder was packed in tube-in-tube hollow fiber membranes to eliminate the problems of recovery and secondary pollution. The effects of one pass-through adsorption and cyclic adsorption in the adsorption of cesium ion were explored. In the one pass-through adsorption, the solution contacts with the adsorbent layer for a short time, resulting in a low adsorption capacity. For the cyclic adsorption, the adsorption capacity can reach 36.26 mg g^{-1}. With the increase of PES inner hollow fiber membranes, the flux increases while the adsorption capacity decreases. The permeation of solution through the PB layer favors the mass transfer of ion to the adsorbent. The tube-in-tube adsorption can solve the recovery problem of PB powder and also improve the adsorption efficiency.

Keywords: Prussian blue; Tube-in-tube hollow fiber membranes; Cesium; Adsorption; One pass-through adsorption; Cyclic adsorption

1. Introduction

Nuclear wastewater has serious influences on human health and ecological environment [1]. In 2011, the Fukushima Daiichi nuclear accident caused widespread contamination, with extreme levels of radionuclides in the environment. Among these radioactive elements, ^{137}Cs is a strong gamma emitter. Due to its long half-life, ^{137}Cs is recognized as the most problematic isotope of cesium in liquid contaminants [2]. The high solubility of cesium causes it migrating to the biosphere via water. In addition, it binds easily to terrestrial and aquatic organisms because of its chemical similarity to potassium [3]. Meanwhile, under natural conditions, cesium exists in the salt lake, geothermal water and oil field brine[1]. The separation of cesium from the natural water is also important for utilizing cesium.

The treatment methods of radioactive wastewater include chemical precipitation, [4] solvent extraction, [5] evaporation and ion exchange [6]. Chemical precipitation is simple in operation, but its selectivity is poor [7]. Solvent extraction also faces the problem of low selectivity [8]. The energy consumption of evaporation method is high [9]. Ion exchange technology is an advanced technologies due to its excellent selectivity, high efficiency and easy operation, [10,11] and has attracted extensive attentions [12,13]. As the first synthetic coordination compound, Prussian blue (PB) has the advantages of simple synthesis, low-cost and

* Corresponding authors.

good stability [14,15]. Ishizaki et al. [16] proposed that the mechanism of adsorption of Cs^+ by Prussian blue is proton exchange, that is, Cs^+ ions are chemically adsorbed on the defect sites of hydrophilic lattice, and exchange with the protons of the coordination water. Nevertheless, Prussian blue particles are small in size and may cause recovery problem and secondary pollution to water bodies [17,18]. Therefore, immobilization of PB is usually employed, but these methods also face the problem of decreased adsorption sites and increased mass transfer resistance. To solve these problems, in this article, PB powder was packed in tube-in-tube hollow fiber membranes. This novel design employs PB powder as absorbent with high loading and low internal diffusion resistance, eliminating the problems of PB recovery and secondary pollution. The effects of one pass-through adsorption and cyclic adsorption modes on the adsorption were studied.

2. Experimental

2.1. Materials

Potassium ferrocyanide, ferric chloride, and concentrated hydrochloric acid were purchased from Beijing Chemical Plant. PTFE, PES, and PVDF hollow fiber ultrafiltration membranes (Molecular weight cut-off of 15,000–20,000) were provided by Solvay Company. Salt lake brine was provided by Qinghai Salt Lake Co., Ltd., and the concentration of Li, Na, K, Rb and Cs is 5,488; 1,879.5; 763.5; 0.0331 and 0.0305 mg L^{-1}, respectively.

2.2. Preparation of PB

200 mL 0.04 mol L^{-1} $FeCl_3$ solution containing 1.6 mol L^{-1} hydrogen chloride acid was prepared. Then 20 mL 0.2 mol L^{-1} $K_4Fe(CN)_6$ solution was added in the $FeCl_3$ solution drop by drop. After stirring vigorously for 2 h, aging for 24 h, washing with deionized water for three times, and drying in vacuum at 80°C for 12 h, the Prussian blue powder was obtained.

2.3. Preparation of tube-in-tube hollow fiber membranes

PES hollow fiber membranes with an outer diameter of 1 mm and PTFE hollow fiber membranes with an inner diameter of 5 mm were used to prepare the tube-in-tube hollow fiber membranes. Prussian blue particles were filled between the two membranes tubes as adsorbent (Fig. 1), and both ends of the fibers were sealed with epoxy resin.

2.4. Adsorption study

In the one pass-through adsorption, as shown in Fig. 2a, the solution first penetrated through PTFE membranes and then the Prussian blue layer, and lastly the PES hollow fiber membrane. The fluxes and the cesium concentration of the permeate were measured. In the cyclic adsorption, as shown in Fig. 2b, the tube-in-tube hollow fiber membranes was immersed in cesium solution, and the solution first penetrated through the PTFE membranes, and then the Prussian blue layer and the PES hollow fiber membrane, and lastly returned to the solution tank. The samples were taken at 1, 3 and 5 h, respectively, and the cesium concentration was determined. For comparison, stirring adsorption was also conducted by adding the same amount of PB in the same volume of cesium solution, and adsorbed for 4 h under stirring. The solution was centrifuged, and the concentration of cesium was determined.

2.5. Characterization

The phase structure of Prussian blue was analyzed by XRD (XRD-7000 Shimadzu, Japan), and the morphology of Prussian blue powder was observed by scanning electron microscope (S-4800 Hitachi High Technology). The cesium concentration was determined by ICP-MS (NEXION300X).

3. Results and discussion

3.1. Characterization of PB powder

XRD analysis of the prepared PB powder showed that there were diffraction peaks at 17.6°, 24.8°, 35.4°, 39.9°, 43.7°, 50.9°, 54.2° and 57.5° (Fig. 3a), corresponding to 200, 220, 400, 420, 422, 440, 600 and 620 crystal planes. It belongs to cubic crystal and Fm3m space group, which is consistent with literature [19]. According to Scheller's formula [20],

$$D = \frac{k\gamma}{B\cos\theta} \tag{1}$$

where D is the average grain size, K is the Scherrer constant, γ is the X-ray wavelength, B is the half-height width of the diffraction peak, and θ is the Bragg diffraction angle. The calculated crystalline grain is about 45 nm in size. SEM showed that PB particles are irregular and polydispersed in size (Fig. 3b).

3.2. One pass-through adsorption

In the one pass-through adsorption with the tube-in-tube hollow fiber membranes, 1.71 g Prussian blue powder were filled between the two hollow fiber membranes (12 cm in length, outer membrane area of 18.84 cm^2, packing density of 0.19 g cm^{-3}).100 mL brine was filtered and

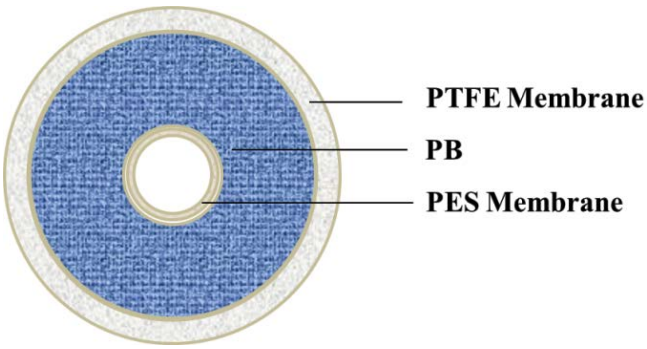

Fig. 1. Tube-in-tube hollow fiber membranes.

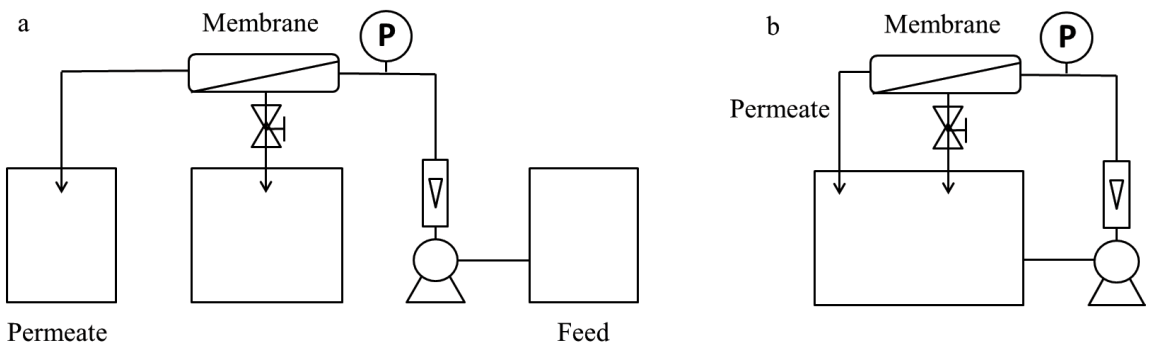

Fig. 2. (a) Diagram of one pass-through adsorption and (b) diagram of cyclic adsorption of cesium chloride solution.

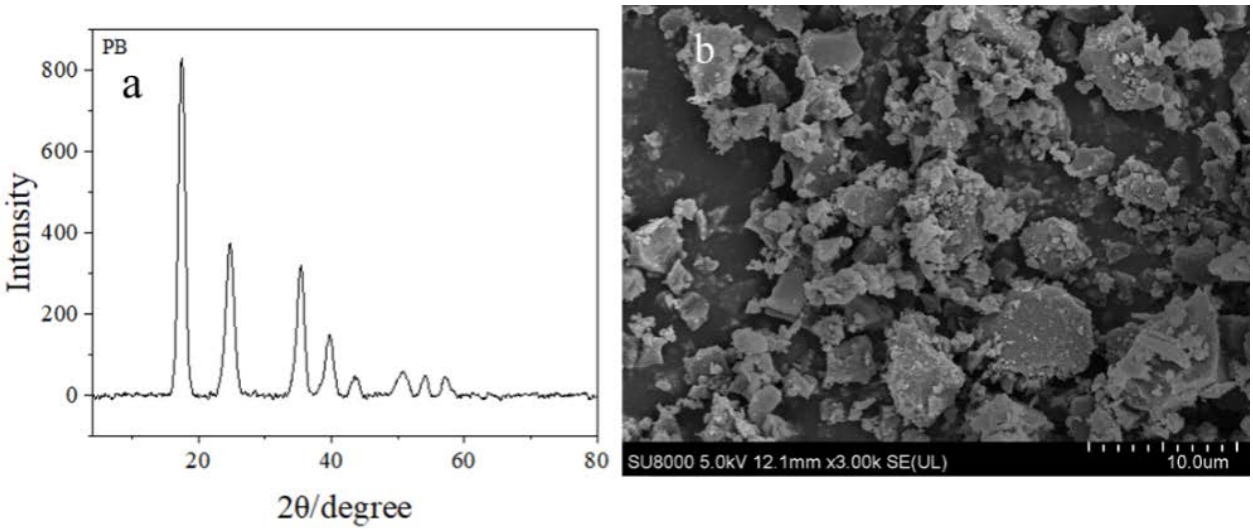

Fig. 3. (a) XRD spectra of PB and (b) SEM of PB powder.

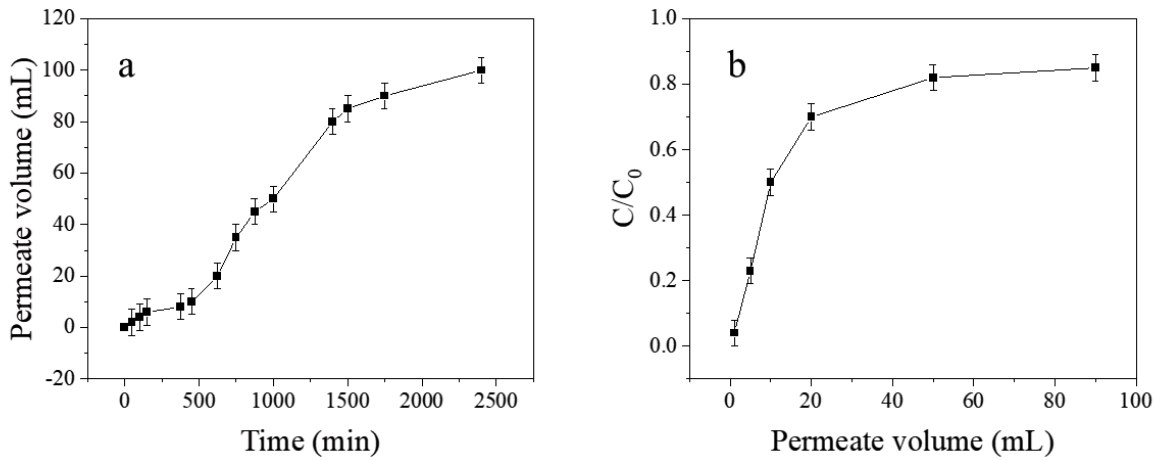

Fig. 4. One pass-through adsorption (a) volume-time curve and (b) dynamic filtration curve.

the filtrate was collected for concentration determination. The penetration rate is slow in the first 400 min, and then increases and tends to be stable, with average flux of 26.54 L h^{-1} m^2 bar^{-1}. Then, the penetration rate slows down due to membrane fouling (Fig. 4a). When the permeate volume is less than 30 mL, C/C_0 increases significantly (Fig. 4b). C/C_0 = 0.1 is the penetration point, and C/C_0 = 0.8 is the saturation point. The penetration volume

V_b is 2.08 mL (V_1/V_{PB} = 0.3, and V_1 and V_{PB} are the volume of permeate and PB bed, respectively), and the saturation volume V_s is 20.00 mL (V_1/V_{PB} = 5.6). The dynamic adsorption capacity (DC) at 0.1 C_0 and 0.8 C_0 is expressed as,

$$\mathrm{DC} = \frac{\int_0^V (C_0 - C)dV}{W_0} \tag{2}$$

where V (L) is the permeate volume, C_0 (mg L^{-1}) is the initial concentration of cesium, C (mg L^{-1}) is the cesium concentration in the permeate, and W_0 (g) is the mass of Prussian blue. The dynamic adsorption capacity DC at 0.1 C_0 and 0.8 C_0 is 0.53 and 3.15 mg g^{-1}, respectively. In the one pass-through adsorption, the residence time of solution in the adsorbent layer is short, resulting in the low dynamic adsorption capacity. Therefore, cyclic adsorption was employed in the following section to enhance the contact time of the adsorbent with the solution.

3.3. Cyclic adsorption of cesium solution

One piece of PES hollow fiber membrane and two pieces of PES hollow fiber membranes were used as inner membranes in the tube-in-tube hollow fiber membranes (6 cm in length, PB loading of 0.31 and 0.24 g, and packing density of 0.067 and 0.053 g cm^{-3}), respectively. First, the pure water permeability was measured. Fig. 5a shows that the permeate volume of pure water displays a linear relationship with the time. The pure water flux is defined as F (L h^{-1} m^{-2} bar^{-1}):

$$F = \frac{V}{t \cdot S \cdot p} \tag{3}$$

where V is the permeate volume, t is the time, S is the area of outer membrane (9.42 cm^2), and P is the pressure. 200 mL of 1 mmol L^{-1} cesium chloride solution was adsorbed by the cyclic adsorption, and the solution concentration was determined at 1, 3 and 5 h by ICP-MS. For comparison, stirring adsorption was also conducted by employing the same amount of PB (0.31 g) in the same volume of solution (200 mL, 1 mmol L^{-1} CsCl).

With the increases time, C/C_0 decreases (Fig. 5c). The dynamic adsorption capacity (DC) is defined as (mg g^{-1}),

$$\mathrm{DC} = \frac{(C_0 - C_X) \cdot V}{m} \tag{4}$$

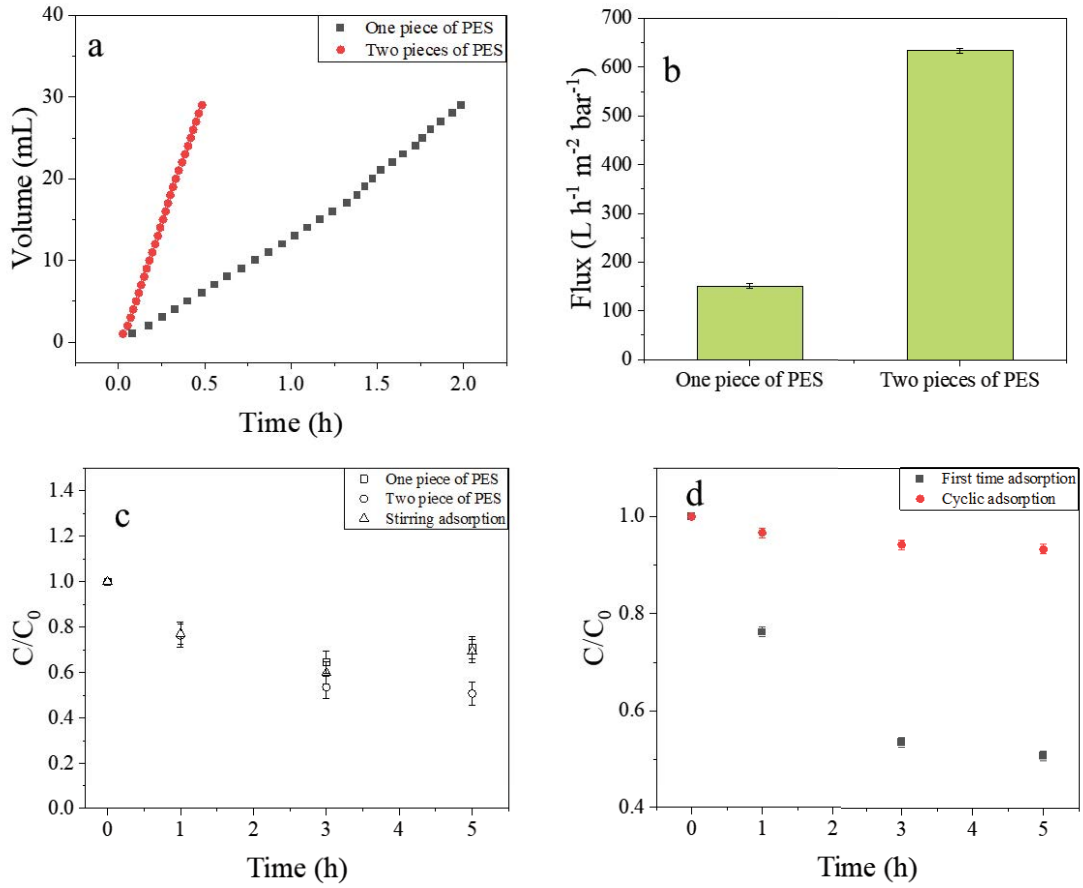

Fig. 5. Cyclic adsorption (a) volume-time curve, (b) the flux, (c) ratio of residual cesium concentration to the initial concentration (The solution in the pipes in the cycling adsorption may result in errors of concentration data), and (d) regeneration and reuse of membranes.

where C_0 (mg L^{-1}) is the initial concentration of cesium, C_X (mg L^{-1}) is the cesium concentration after adsorption, V (L) is the solution volume, and m (mg) is the mass of PB. The adsorption capacity of tube-in-tube hollow fiber membranes with one piece of PES membranes is 36.26 mg g^{-1} at 5 h. This value is higher than those with two pieces of PES membranes (32.68 mg g^{-1}) and the stirring adsorption (33.31 mg g^{-1}). The increased pieces of PES inner hollow fiber membranes in the PTFE outer hollow fiber membrane results in less PB filled and then lower adsorption capacity. In the tube-in-tube hollow fiber membranes, the solution permeates through the PB layer, and the convection flow improves the mass transfer of ion to the adsorbent, resulting in higher adsorption capacity than that of the stirring adsorption. Thus, the tube-in-tube adsorption can not only solve the recovery problem of PB, but also improve the adsorption efficiency. Hu et al. [21] prepared polyurethane foam quaternary composites containing Prussian blue, diatomite and carbon nanotubes by growing Prussian blue in situ on diatomite, and the removal rate of 40 mL 100 mg L Cs^+ solution can reach 90.62% when the dosage of 150 g is added in adsorption. In comparison, in this work, nearly 50% removal is attained for adsorption of 200 mL of 250 mg L^{-1} Cs^+ solution with the dosage of 0.3 g, reflecting the efficiency of tube-in-tube hollow fiber membranes adsorption. For adsorption of radionuclide ^{137}Cs, regeneration of membranes is not required, and the used membranes can be stored underground. For adsorption of nonradioactive Cs, regeneration of membranes is needed. 100 mL of 0.5 mol L^{-1} NH_4Cl solution was used for cyclic elution of the tube-in-tube hollow fiber membranes for 5 h. The elution rate was calculated to beover 75%.

3.4. Cyclic adsorption of salt lake brine

The tube-in-tube hollow fiber membranes with one piece of PES inner membranes (6 cm in length, PB loading of 0.31 g) was also employed in the cyclic adsorption of salt lake brine (100 mL, concentration of Li, Na, K, Rb and Cs of 5,488; 1,879.5; 763.5; 0.0331 and 0.0305 mg L^{-1}, respectively), and the brine concentration was analyzed at 12 h and 24 h for ICP test. It is found that the concentration of cesium decreases with time (Fig. 6a). The pseudo-first-order and pseudo-second-order kinetic models were used to fit the PB adsorption. The pseudo-first-order adsorption kinetics is expressed as [22]:

$$\log\left(Q_e - Q_t\right) = \log Q_e - \frac{k_1 t}{2.303} \tag{5}$$

where Q_e is the equilibrium adsorption capacity of adsorbent for cesium (mg g^{-1}), Q_t is the adsorption capacity at time t (mg g^{-1}), k_1 is the first-order adsorption rate constant (min^{-1}). The pseudo-second-order adsorption kinetics is expressed as follows,

$$\frac{t}{Q_t} = \frac{1}{k_2 Q_e^2} + \frac{t}{Q_e} \tag{6}$$

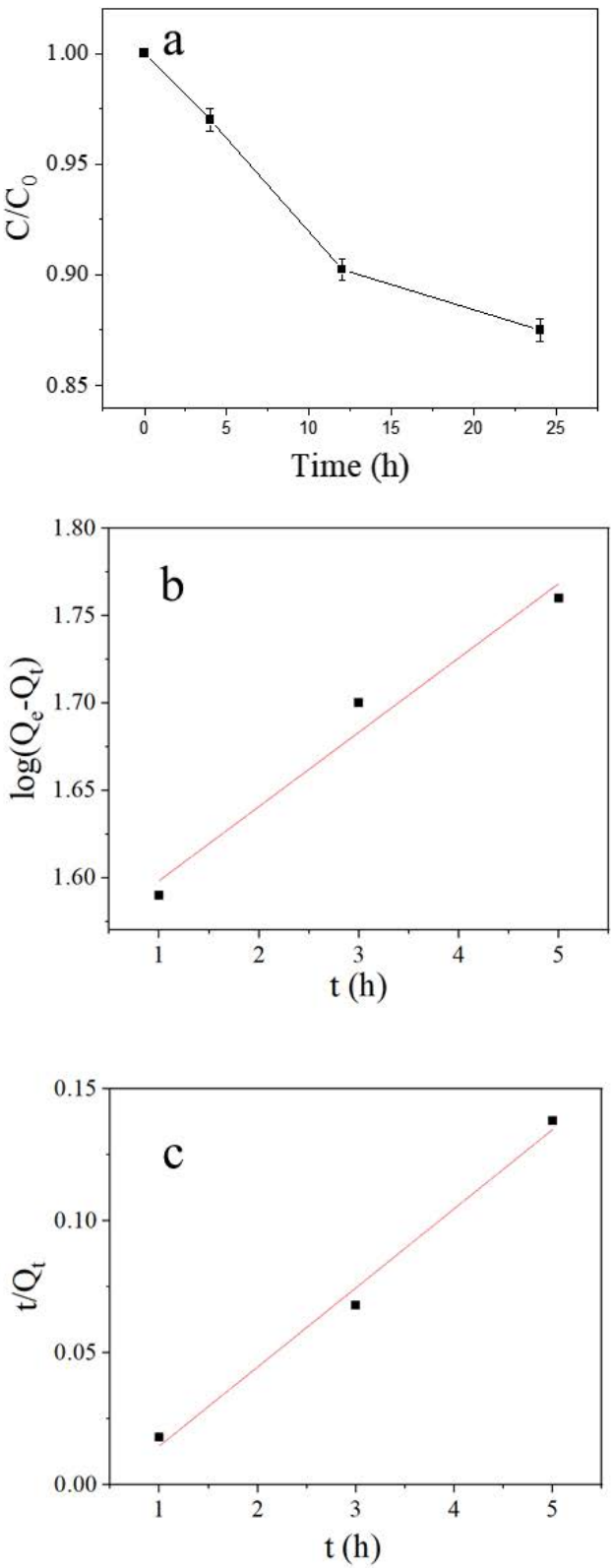

Fig. 6. Cyclic adsorption with one of PES inner membrane (a) salt lake brine adsorption, (b) fitting of pseudo-first-order dynamics model, and (c) fitting of pseudo-second-order dynamics model.

Table 1
Kinetic parameters of cesium adsorption by casing membranes

Kinetic models	Parameter	Parameter value
Pseudo-first-order	Slope	0.043
	Intercept	1.56
	k_1 (min^{-1})	0.10
	R^2	0.97
Pseudo-second-order	Slope	0.011E-17
	Intercept	4.16E-17
	k_2 (g mg^{-1} min^{-1})	65.37
	R^2	0.99

where k_2 is the second-order adsorption rate constant (g mg^{-1} min^{-1}). Fig. 6b shows the linear fitting of $\log(Q_e - Q_t)$ to t, and Fig. 6c shows the linear fitting of t/Q_t to t, and the fitting parameters are shown in Table 1. The results show that pseudo-second-order adsorption kinetics can better describe the adsorption kinetics ($R^2 > 0.99$), and k_2 is 65.37 g mg^{-1} min^{-1}, indicating that chemisorption process is a rate control step.

4. Conclusions

Tube-in-tube hollow fiber membranes adsorption was explored. In the one pass-through adsorption, the residence time of solution in the adsorbent layer is short, resulting in low dynamic adsorption capacity. In the cycling adsorption, the increased pieces of PES inner hollow fiber membranes in the PTFE outer hollow fiber membranes results in greater flux, less PB filled and lower adsorption capacity. The permeation of solution through the PB layer favors the mass transfer of ion to the adsorbent. The tube-in-tube adsorption solves the recovery problem of PB powder, and also improve the adsorption efficiency.

Acknowledgements

This work was supported by the National Natural Science Foundation of China (No. 51920105012), and the National Natural Science Foundation of China and Qinghai Qaidam Saline Lake Chemical Science Research Joint Fund (No. U1607109).

References

[1] Z. Jia, X.Cheng, Y. Guo, L. Tu, *In-situ* preparation of iron(III) hexacyanoferrate nano-layer on polyacrylonitrile membranes for cesium adsorption from aqueous solutions, Chem. Eng. J., 325 (2017) 513–520.
[2] Y. Kim, Y.K. Kim, S. Kim, D. Harbottle, J.W. Lee, Nanostructured potassium copper hexacyanoferrate-cellulose hydrogel for selective and rapid cesium adsorption, Chem. Eng. J., 313 (2016) 1042–1050.
[3] A. Nilchi, R. Saberi, M. Moradi, H. Azizpour, R. Zarghami, Adsorption of cesium on copper hexacyanoferrate–PAN composite ion exchanger from aqueous solution, Chem. Eng. J., 172 (2018) 572–580.
[4] S.G. Beheir, K. Benyamin, F.M. Mekhail, Chemical precipitation of cesium from waste solutions with iron(II) hexacyanocobaltate(III) and triphenylcyanoborate, J. Radioanal. Nucl. Chem., 232 (1998) 147–150.
[5] A. Casnati, R. Pochini, R. Ungaro, F. Ugozzoli, F. Arnaud, S. Fanni, M. Schwing, R.J.M. Egberink, F. Jong, D.N. Reinhoudt, Synthesis, complexation, and membrane transport studies of 1,3-alternate calix[4]arene-crown-6 conformers: a new class of cesium selective ionophores, J. Am. Chem. Soc., 117 (1995) 2767–2777.
[6] T.Y. Kim, S.S. An, W.G. Shim, J.W. Lee, S.Y. Cho, J.H. Kim, Adsorption and energetic heterogeneity properties of cesium ions on ion exchange resin, J. Ind. Eng. Chem., 27 (2015) 260–267.
[7] J. Wang, S. Zhuang, Removal of cesium ions from aqueous solutions using various separation technologies, Rev. Environ. Sci. Biotechnol., 18 (2019) 231–269.
[8] E. Makrlík, P. Vaňura, P. Selucký, Solvent extraction of cesium into nitrobenzene by using hydrogen dicarbollylcobaltate and dodecaethylene glycol, J. Radioanal. Nucl. Chem., 297 (2013) 115–118.
[9] D. Guery-Odelin, J. Soeding, P. Desbiolles, J. Dalibard, Strong evaporative cooling of a trapped cesium gas, Opt. Express, 2 (1998) 323–329.
[10] C. Sun, F. Zhang, J. Cao, A 'build-bottle-around-ship' method to encapsulate ammonium molybdophosphate in zeolite Y. An efficient adsorbent for cesium, J. Colloid Interface Sci., 455 (2015) 39–45.
[11] Z. Jia, S. Hao, X. Cheng, X. Lu, L. Tu, Fabrication of Prussian blue/polydopamine layers on polyacrylonitrile membranes for efficient adsorption of cesium, Desal. Water Treat., 163 (2019) 125–132.
[12] S. Hao, Z. Jia, J. Wen, S. Li, W. Peng, R. Huang, X. Xu, Progress in adsorptive membranes for separation – a review, Sep. Purif. Technol., 255 (2021) 117772–117780.
[13] E. Cho, J.J. Lee, B. Lee, K. Lee, B. Yeom, T.S. Lee, Cesium ion-exchange resin using sodium dodecylbenzenesulfonate for binding to Prussian blue, Chemosphere, 244 (2020) 125589–125597.
[14] J. Qian, S. Cai, S. Yang, D. Hua, A thermo-sensitive polymer network crosslinked by Prussian blue nanocrystals for cesium adsorption from aqueous solution with large capacity, J. Mater. Chem. A, 5 (2017) 22380–22388.
[15] Z. Jia, G. Sun, Preparation of prussian blue nanoparticles with single precursor, Colloids Surf., A, 302 (2007) 326–329.
[16] M. Ishizaki, S. Akiba, A. Ohtani, Y. Hoshi, K. Ono, M. Matsuba, T. Togashi, K. Kananizuka, M. Sakamoto, A. Takahashi, T. Kawamoto, H. Tanaka, M. Watanabe, M. Arisaka, T. Nankawa, M. Kurihara, Proton-exchange mechanism of specific Cs^+ adsorption via lattice defect sites of Prussian blue filled with coordination and crystallization water molecules, Dalton Trans., 42 (2013) 16049–16055.
[17] J. Huo, G. Yu, J. Wang, Selective adsorption of cesium(I) from water by Prussian blue analogues anchored on 3D reduced graphene oxide aerogel, Sci. Total Environ., 761 (2021) 143286–143306.
[18] Z. Jia, Synthesis of Prussian Blue nanocrystals with metal complexes as precursors: quantitative calculations of species distribution and its effects on particles size, Colloids Surf., A, 389 (2011) 144–148.
[19] A.M. Farah, N.D. Shooto, F.T. Thema, J.S. Modis, E.D. Dikio, Fabrication of prussian blue/multi-walled carbon nanotubes modified glassy carbon electrode for electrochemical detection of hydrogen peroxide, Front. Chem., 7 (2012) 4302–4313.
[20] D.J. Lim, N.A. Marks, M.R. Rowles, Universal Scherrer equation for graphene fragments, Carbon, 162 (2020) 475–480.
[21] B. Hu, B. Fugetsu, H. Yu, Y. Abe, Prussian blue caged in spongiform adsorbents using diatomite and carbon nanotubes for elimination of cesium, J. Hazard. Mater., 217 (2012) 85–91.
[22] Y. Guo, Z. Jia, Novel sandwich structure adsorptive membranes for removal of 4-nitrotoluene from water, J. Hazard. Mater., 317 (2016) 295–302.